SP 188-94

Bond Splitting Behavior of Continuous Fiber Reinforced Concrete Members

by T. Sakai, T. Kanakubo, K. Yonemaru, and H. Fukuyama

Synopsis:

For the purpose of investigating the bond splitting behavior of continuous fiber reinforced concrete (CFRC) members, two series of investigations were conducted. The first series was performed in order to obtain the local bond behavior in the case of splitting failure of the concrete cover for members with or without lateral reinforcements. For specimens without lateral reinforcement, test results show that the bond splitting strength is not influenced by the Young's modulus of the reinforcement and that it is approximately proportional to the thickness of the cover concrete. On the other hand, for specimens with lateral reinforcement, the local bond splitting strength is greater than the case where there is no lateral reinforcement. The strength is also independent of the mechanical property of the lateral reinforcement and is determined solely by the thickness of concrete cover. For both types, a new relationship between the bond stress (τ) and the slip of reinforcements (s) is proposed.

The second series was an analytical study to investigate the average bond behavior of CFRC members, which had several bond lengths and Young's moduli. Analytical results show that in the case of large bond lengths, the analytical bond splitting strength is inversely proportional to the bond length, and is clearly influenced by the Young's modulus of the reinforcement. It is considered that continuous bond failure from the loaded end causes a remarkable decrease in the bond strength especially for large bond lengths and low Young's moduli.

Keywords: bond splitting; concretes; continuous fiber; reinforced concrete

Takahiro Sakai is a graduate student of doctoral program of University of Tsukuba, Japan.

Toshiyuki Kanakubo, Dr.E. is an Assistant Professor of Institute of Engineering Mechanics, University of Tsukuba, Japan.

Keisuke Yonemaru, ME, is a Research Engineer of Institute of Technology, Shimizu Corporation, Japan.

Hiroshi Fukuyama, Dr.E. is a Senior Research Engineer of Building Research Institute, Ministry of Construction, Japan.

INTRODUCTION

In recent years, research involving the use of Fiber Reinforced Plastic Reinforcement (FRPR) as the main reinforcement in concrete is being conducted frequently, especially, bond splitting experimental tests. Experimental results on the cantilever specimens having a bond length of 23 times the main bar diameter show that the length of the stressed portion on the FRPR bar is about 10 times the main bar diameter (1). It is also considered that a low Young's modulus causes the bond splitting failure from the loaded end to be of the continuous failure type and that the length of the bond stress acting could be influenced by Young's modulus of the reinforcement. Young's modulus of FRPR could be varied by the material, surface configuration and so on.

To investigate the relationship between bond splitting strength and Young's modulus of reinforcement or bond length of the specimen, the bond splitting test was conducted with FRPR as a main bar.

BOND SPLITTING STRENGTH ACCORDING TO TEPFERS

Tepfers (2) presented the bond splitting strength by modeling the stress condition of the surrounding concrete around the loaded main bar to the internal stresses present inside a cylinder (Fig. 1). The tensile stress, σ_θ, acting at a radius, r, from the main bar in a hollow cylinder with an inner radius, r_i, and outer radius, r_u, having an inner stress, σ, is given by eq.[1] according to Timoshenko (3).

If it is assumed that the bond splitting occurs when the tensile stress, σ_θ, equals the splitting strength of the concrete, σ_t, at a distance equal to the inner radius, r_i, the internal stress, σ, can be represented in eq.[2]. As shown in Fig. 1, the resulting stresses made when the main bar pushes against the surrounding concrete is composed of the lateral component, σ_s, and the bond stress along the direction of the main bar, τ_b, and whose relation is given in eq.[3]. Also, assuming equilibrium of the compressive forces acting inside cracked inner portion of the cylinder, the relationship between σ_s and σ can be represented in eq.[4]. Thus, by substituting eq.[3] and eq.[4] into eq.[2], the bond stress is given by eq.[5]. By

differentiating τ_b by r_i, the maximum value of the bond stress is derived as given in eq.[6].

$$\sigma_\theta = \sigma \cdot \frac{r_i^2}{r_u^2 - r_i^2}\left(1 + \frac{r_u^2}{r^2}\right) \quad [1] \qquad \sigma = \sigma_t \cdot \frac{r_u^2 - r_i^2}{r_u^2 + r_i^2} \quad [2]$$

$$\tau_b = \sigma_s \cdot \cot\alpha \quad [3] \qquad \sigma_s \cdot \pi \cdot d_b = \sigma \cdot \pi \cdot 2r_i \quad [4]$$

$$\tau_b = \sigma_t \cdot \frac{2r_i}{d_b} \cdot \frac{r_u^2 - r_i^2}{r_u^2 + r_i^2} \cdot \cot\alpha \quad [5]$$

$$\tau_{b,max} = 0.6006 \cdot \sigma_t \cdot \frac{r_u}{d_b} \cdot \cot\alpha \quad [6]$$

EXPERIMENTAL TEST

Test Program

To obtain the local bond behavior in the case of splitting failure of the cover concrete, an experimental test was conducted.

As shown in Fig. 2, specimens with a bond length of four times the diameter of the reinforcement were tested. Slits on four or two sides of each of the specimens were designed in order to fail by concrete splitting along the slits. Thickness of the cover concrete (C) is varied by length of the slit. Two types of specimens were designed. One is for specimen without lateral reinforcement (hereafter called Type A), and the other is for specimen with lateral reinforcement (called Type B). Type B specimens, one main bar was positioned at the center of the specimen and also, a single bent bar was arranged in a manner representative of the bar arrangement in a structural member. The portion of the lateral reinforcement lying along the loading direction is unbonded.

A monotonic tensile load was applied until failure occurred. In Type B specimens, proportional tensile load to main bar load was applied by two oil jacks. The measured items were the tensile load and the slip of the free end of the main bar.

In Type A specimens, different types of reinforcement were used as main bars, namely, ordinary steel (diameters of 13, 16, 19 and 25mm), carbon and glass (diameter of 16mm). For the carbon bar, two types were used, wherein either carbon or glass were coiled around the surface of the carbon bar. On the other hand, in Type B specimens, different types of reinforcement were for the lateral bars, ordinary steel (diameters of 4, 6, and 8mm), carbon, glass (diameter of 6mm) and aramid (diameter of 6mm). Mechanical properties for each of the reinforcements are shown in Table 1.

In Type A specimens, design compressive strength of 36MPa concrete, and in Type B specimens, design compressive strength of 20, 30 and 45MPa concrete were cast. The material test results are shown in Table 2.

Test results show that almost all the specimens failed by concrete splitting toward the slits (Photo 1). The maximum bond stress was derived by dividing the maximum load by the surface area of main bar.

Influence of the parameters on the bond behavior in case of no lateral bar : For this experiment, considering the type of reinforcement used, focus is made in the value of their Young's moduli. Therefore, a relationship between different values of the Young's modulus and the resulting bond splitting behavior is investigated as shown in Fig. 3. For this case, the values of the bond strength and slip are determined. The bond splitting strength is derived by the maximum bond stress divided by splitting strength of concrete. Fig. 3 shows that both bond strength and load end slip are not influenced by the variation of the Young's modulus of the reinforcement.

In investigating the influence of the thickness of the cover concrete, a relationship between r_u/d_b ($=C/d_b+0.5$) and bond splitting strength is shown in Fig. 4 using a straight line plot derived from regression analysis. In the figure, the specimens are classified into the two types of the reinforcement, steel and fiber. Results show that the bond splitting strength is proportional to r_u/d_b as could be shown in eq.[6], in spite of type of reinforcement. The determination of the value of $\cot \alpha$ was done by using eq.[6] with the experimental results. The average calculated $\cot \alpha$ for all specimens was 1.47, where α was 34 degrees.

Influence of the parameters on the bond behavior with lateral bar : Fig. 5 shows the relationship between the Young's modulus and cross-sectional area of the lateral reinforcement and the bond splitting strength. Marks were changed for each type of lateral reinforcement. From both figures, it is observed that there is no clear trend showing that the influence given by the difference in the types of lateral reinforcement is negligible. Fig. 6 shows the relationship between the concrete cover and the bond splitting strength. The value of eq.[6] (α:34 degrees) is represented by the straight line. the bond splitting strength tends to increase as concrete cover increases. And the

experimented values are greater than the calculated value. However, the amount of increase is not so large that, the difference in the types of lateral reinforcement and concrete cover is not so emphasized.

RELATIONSHIP BETWEEN THE BOND STRESS AND THE SLIP OF THE REINFORCEMENT

Basic Equation of the Slip of the Reinforcement in Bond behavior

Consider an infinitesimal element Δx at arbitrary position of the main reinforcement, slip of the reinforcements, tensile force of the reinforcement P, tensile stress σ, strain of the reinforcement ε, and bond stress τ_b to be determined. These parameters could have the following relationships.

$$dP = \tau_b \cdot \phi_b \cdot dx \qquad [7] \qquad dP = d\sigma_b \cdot a_b \qquad [8]$$

$$d\sigma_b = E_b \cdot d\varepsilon_b \qquad [9] \qquad ds = d\varepsilon_b \cdot dx \qquad [10]$$

where, ϕ_b : perimeter of the reinforcement
a_b : cross-sectional area of the reinforcement
E_b : Young`s modulus of the reinforcement

By using eq.[7]~eq.[10], the following eq.[11] and eq.[12] could be presented.

$$\frac{ds}{dx} = \frac{P}{E_b \cdot a_b} \qquad [11] \qquad \frac{d^2 s}{dx^2} = \frac{\phi_b}{E_b \cdot a_b} \cdot \tau_b \qquad [12]$$

Relationship between the Slip of the Reinforcement

If some relationship between the inner radius, r_i and the slip, s could be derived, τ_b can be shown as a function of s by eq.[5]. In investigating the relationship between r_i and s, r_i was determined by computer calculation with the substitution of the experimental bond stress in eq.[5]. A typical example of the relation between the calculated r_i and loaded end slip s is shown in Fig. 7 (specimens using steel bars). This shows that r_i is almost proportional to loaded end slip. To determine the proportionality constant, a relationship between the constant and the diameter of the reinforcement is needed and is as shown in Fig. 8. From which, eq.[13] is derived, where β

is 10.2. By substituting eq.[13] into eq.[5], the bond stress τ_b could be represented in eq.[14].

$$r_i = \beta \cdot d_b \cdot s \qquad [13]$$

$$\tau_b = 2 \cdot \sigma_t \cdot \beta \cdot s \cdot \frac{(r_u/d_b)^2 - (\beta \cdot s)^2}{(r_u/d_b)^2 + (\beta \cdot s)^2} \cdot \cot\alpha \qquad [14]$$

Construction of a Model for the case with Lateral Reinforcement

Eq.[14] shows the relationship between the bond stress and loaded end slip of the case without lateral reinforcement. And Fig. 9 shows a example of the relationship between the bond stress and loaded end slip obtained using this experimental test for the case with lateral reinforcement, as well as the relationship between the bond stress and loaded end slip obtained by eq.[14]. To construct a model for the case with lateral reinforcement, emphasis is given to the increase in the amount of the bond strength τ_{inc} as represented by the shaded portion in the figure. The increase in the amount of the bond stress is defined as the difference between the experimental results using specimens with lateral reinforcement and theoretical results using eq.[14].

The left graph of Fig. 10 shows the example of the relationship between the increment of bond stress and loaded end slip defined in the previous paragraph. Here, the model of the relationship between the bond stress and loaded end slip is defined by two straight lines as shown in the right graph. The first line is the straight line increase from the datum point to the loaded end slip that r_1 becomes r_u ($r_1 = r_u$), and takes the maximum value τ_{incmax} that is equal to the concrete cover (r_u)

Fig. 11 shows the relation between values of slope, k_1 and k_2, and lateral reinforcement ratio. Both values are standardized by concrete splitting strength. As shown in the figures, the value of first slope k_1 is almost constant, and the value of second slope k_2 is inversely proportional to lateral reinforcement ratio.

ANALYSIS FOR AVERAGE BOND BEHAVIOR

The Method of Analysis

The following step-by-step procedure is presented to obtain the average bond behavior such as acting in actual members using constructed bond stress – slip model. First, consider an its infinitesimal element Δx at arbitrary position of the main reinforcement, and at free end, the amount of slip s_{i-1} (= free end slip s_0) and the tensile force of the reinforcement ΔP_{i-1} (=0) is determined. Second, for each element, determine the bond stress using the model. And since Δx could be considered as very small, the bond stress could be assumed as constant. The difference in the tensile force ΔP_i and the amount of slip Δs_i at the infinitesimal element could be given by eqs.[15] and [16]. Lastly, the amount of slip at the other end of the infinitesimal element s_i and the tensile force of the reinforcement P_i could be represented by eqs.[17] and [18]. These procedure is conducted iteratively. Also, the determination of the average bond stress by dividing the calculated P_i at the loaded end with the perimeter of the main reinforcement and the total bond length is possible.

$$\Delta P_i = \tau_{bi} \cdot \phi_b \cdot \Delta x \qquad [15]$$

$$\Delta s_i = \frac{\Delta x}{E_b \cdot a_b}\left(\sum_{k=0}^{i-1} \Delta P_k + \frac{\Delta P_i}{2}\right) \qquad [16]$$

$$s_i = s_{i-1} + \Delta s_i \qquad [17]$$

$$P_i = \sum_{k=0}^{i} P_k \qquad [18]$$

The Comparison between Analytical Results and Experimental Results

The analytical data adopted for the verification were the specimens having lateral reinforcement, and failed by the side splitting type in Yonemaru's research (4) as shown in Table 3. Fig. 12 shows the comparison between the experimental results and analytical results of the bond splitting strength. In this figure, the analytical results matches favorably with the past experimental results, and good conformity is noticed in the case of long bond lengths.

Influence of the Bond Length to the Bond Strength

The influence on the bond splitting strength by bond length is given in Fig. 13. The analysis was conducted using two types of specimens, namely, carbon and glass as shown in the left and right graphs, respectively. The horizontal axis shows the bond length (divided by diameter of reinforcement, l_b/d_b). In this graph, the analytical result is shown as the solid line, and the dotted line shows the inversely proportional line. Analytical results show that in the case of short bond lengths, the analytical bond splitting strength is given by the maximum local bond stress, while in the case of large bond lengths (larger than about 15 times of diameter), the analytical bond splitting strength is inversely proportional to bond length, and is clearly influenced by the Young's modulus. These results prove that by the continuous splitting failure from the loaded end, the average bond stress tends to decrease as the bond length increases. On the other hand, the bond length of four times the diameter can be appropriate to get local bond behavior by the experiments.

Influence of Young's Modulus of Main Bar

The distribution of the bond stress (solid line) and the tensile load (dotted line) according to the value of the Young's modulus are shown in Fig. 14 and Fig. 15 in case with and without lateral reinforcement, respectively. The reinforcements used are of two types, namely, steel (198GPa) and glass fiber (38.7GPa). The graphs show that, in the case of the lower Young's modulus, the area where bond stresses are acting is small, thus the tensile load at loaded end becomes small.

CONCLUSIONS

1. The Young's modulus of the reinforcement is of little influence to the local bond behavior.
2. A new relationship between the bond stress (τ) and slippage of the reinforcements (s) is proposed.
3. Analytical results show that in the case of large bond length, the analytical bond splitting strength is inversely proportional to the bond length, and is clearly influenced by the Young's modulus.
4. Analytical result indicate the area where bond stresses are acting is small in the case of the lower Young's modulus. The tensile load at loaded end becomes small.

REFERENCES

(1) T. Kanakubo, K. Yonemaru, H. Fukuyama, M. Fujisawa and Y. Sonobe, "Bond Performance of Concrete Members Reinforced with FRP Bars", ACI, Fiber-Reinforced-Plastic Reinforcement for Concrete Structures, SP138, pp.767～788, Nov. 1993

(2) R. Tepfers. "Lapped Tensile Reinforcement Splices", ASCE, Journal of Structural Division, Vol.108, No. ST1, pp.283～301, Jan. 1982.

(3) S. P. Timoshenko and J. N. Goodier Theory of Elasticity, 3rd ed. (International Student Edition), McGraw-Hill Kogakusha Ltd., Tokyo, Japan, 1970

(4) K. Yonemaru, K. Kanakubo, H. Hukuyama and Y. Sonobe, "Bond Splitting Strength of Reinforced Concrete Members with FRP Bars", Concrete Research and Technology, JCI, Vol.4, No.2, pp.101～109, 1993. 7

TABLE 1—MECHANICAL PROPERTIES OF REINFORCEMENT.

Mate -rial	Surface configuration	Name	Cross-sectional area A_b (mm^2)	Diameter d_b (mm)	Perimeter ϕ_b (mm)	Young's modulus E_b (GPa)	Speci men
Steel	Deformed	D4	14.1	4.2	13.3	191.0	TypeB
			15.7	4.47	14.05	181.5	
		D6	30.4	6.2	19.6	176.0	
			31.3	6.31	19.83	189.9	
		D8	59.2	8.7	27.3	185.0	
			45.6	7.62	23.94	186.9	
		SD13	123.1	12.5	39.3	182.4	TypeA
		SD16	192.0	15.6	49.1	185.3	TypeA,B
		SD19	277.2	18.8	59.0	188.2	TypeA
		SD25	499.6	25.2	79.2	197.2	
Carbon	Carbon spiral	CS16	18.4	57.8	265.9	197.1	TypeA
	Glass spiral	CS16G	18.4	57.8	266.3	75.3	
	Straight	C6	33.8	6.6	20.6	60.4	TypeB
Glass	glass spiral	GS16	19.0	59.8	284.2	30.4	TypeA
	Straight	G6	32.3	6.4	20.2	34.4	TypeB
Aramid	Straight	A6	50.7	8.0	25.2	36.1	

TABLE 2—MECHANICAL PROPERTIES OF CONCRETE.

Compressive strength σ_B (MPa)	Splitting strength σ_t (MPa)	Young's modulus E_c (GPa)	Specimen	
36.4	2.83	24.0	SD13,fiber	TypeA
34.3	2.36	24.6	SD16,19,25	
20.1	1.97	22.9	TypeB	
29.3	2.32	24.2		
47.2	3.17	29.2		

TABLE 3—DATA USED FOR VERIFICATION.

Ref.	Number of data	Member Width (cm)	Main bar	Lateral bar	Concrete strength (MPa)	Bond length (cm)	Lateral bar ratio p_w(%)
Yon-emaru et al	38	20	CFRP ϕ 6 GFRP ϕ 13 C128S K128S D13	CFRP ϕ 6,8 GFRP ϕ 6,8 C32,64 K32,64 U5.1	33.04 33.92 34.31	30	0.40 0.78 0.81 1.19

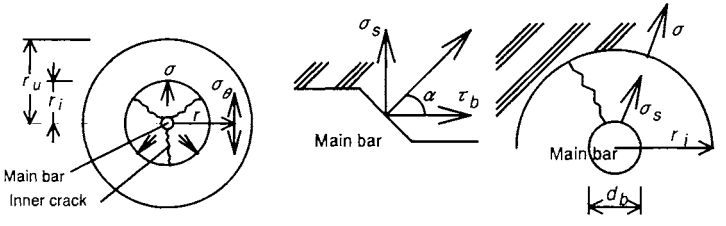

Fig. 1—Internal stress and bond stress.

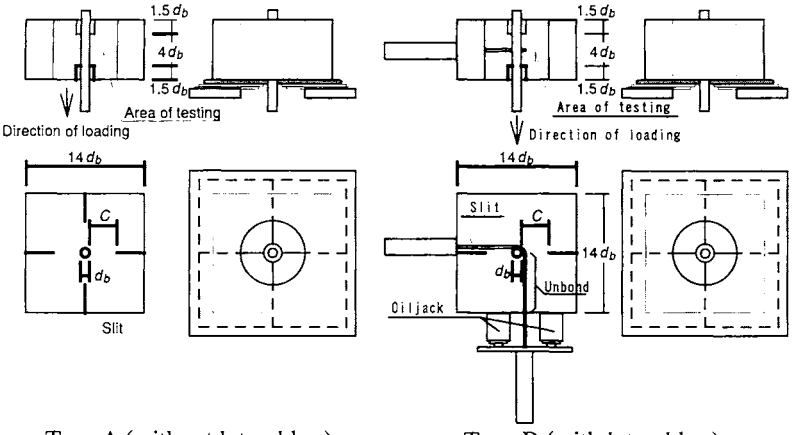

Type A (without lateral bar) Type B (with lateral bar)

Fig. 2—Outline of specimen.

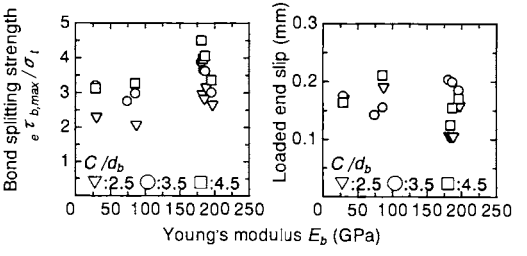

Fig. 3—Relationship between bond behavior and Young's modulus.

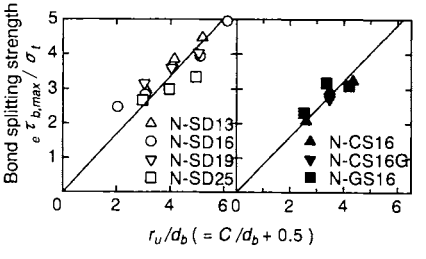

Fig. 4—Relationship between r_u/d_b and bond splitting strength.

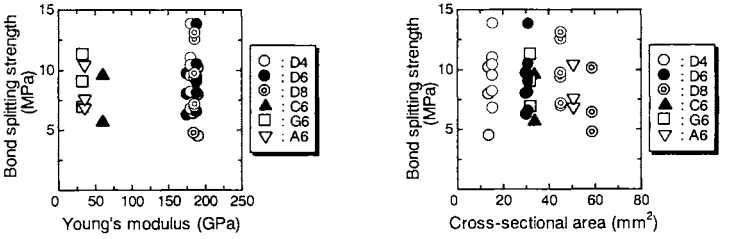

Fig. 5—Influence of Young's modulus and sectional area of lateral reinforcements.

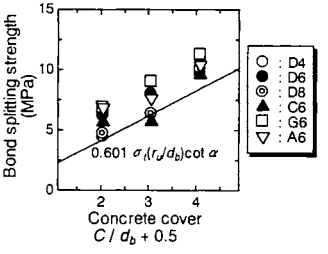

Fig. 6—Influence of concrete cover.

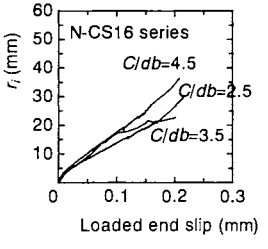

Fig. 7—Relationship between r_i and load end slip.

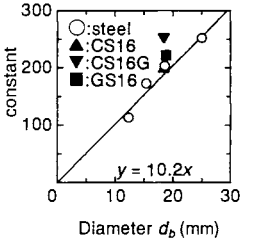

Fig. 8—Determination of proportionality constant β.

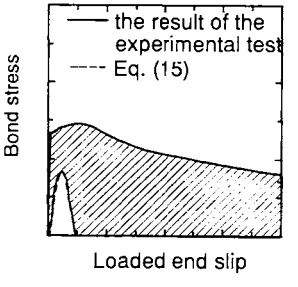

Fig. 9—Example of bond stress: loaded end slip.

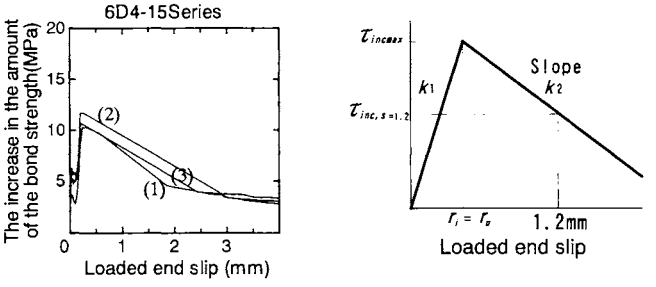

Fig. 10—Increase of bond stress and its model.

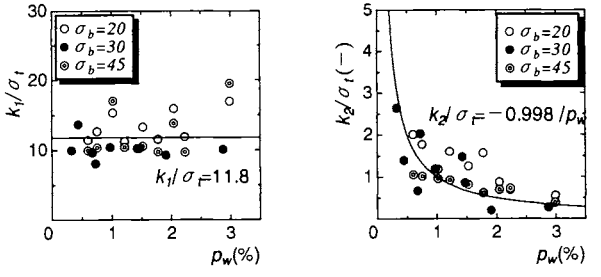

Fig. 11—Relation between values of slope and lateral reinforcement ratio.

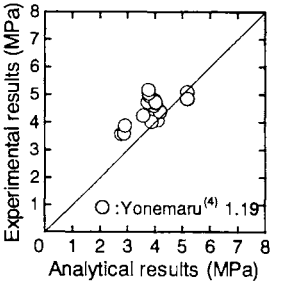

Fig. 12—Verification of analytical results.

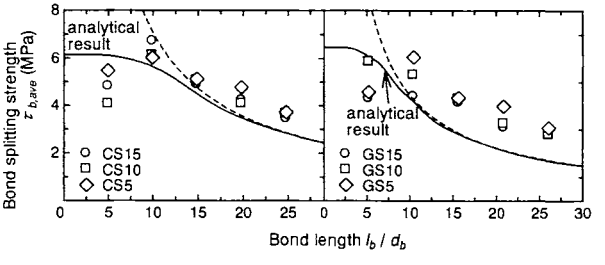

Fig. 13—Relationship between bond length and bond splitting strength.

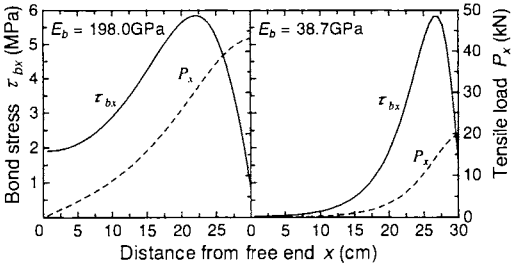

Fig. 14—Distribution of bond stress in case without lateral reinforcement.

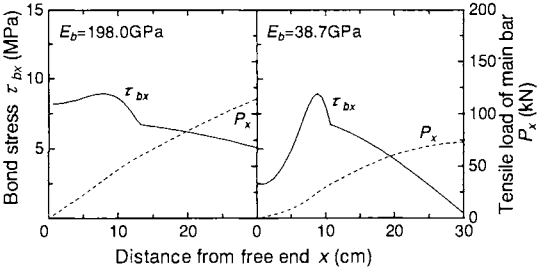

Fig. 15—Distribution of bond stress in case with lateral reinforcement.

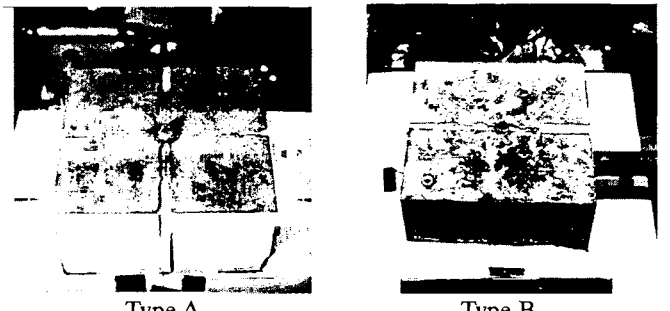

Photo 1—Typical failure type.